Electronic Supplementary Material (ESI) for ChemComm.

Supporting Information

Butterfly Architecture of NIR Aza-BODIPY Small Molecules Decorated with Phenothiazine or Phenoxazine

Ravulakollu Srinivasa Rao [a,b], *B. Yadagiri* [a,b], *Ganesh D. Sharma* [c]*, *Surya Prakash Singh* [ab]*

a) Polymers and Functional Materials Division, CSIR-Indian Institute of Chemical Technology, Uppal Road, Tarnaka, Hyderabad-500007, India

b) Academy of Scientific and Innovative Research (AcSIR), Ghaziabad- 201002, India

c) Department of Physics, The LNMIIT (Deemed University), Jamdoli, Jaipur, Rajstan.302031, India.

***Corresponding Author:** spsingh@iict.res.in

Contents

1. Materials and methods

All the precursor materials were purchased directly from commercial sources and used as such without any further purification and solvents were dried under vacuum by following standard procedure. UV-vis spectrophotometer used to record absorption spectra in dichloromethane (DCM) solution. NMR (^{1}H and ^{13}C) spectra were measured with Advance ACP-400 or AMX2-500 spectrometers at 400 and 500 MHZ respectively, using tetramethylsilane (TMS) as an internal standard. High resolution mass spectra were measured on a Shimadzu LCMS-2010 EV model with ESI probe. Cyclic voltammetry was performed on a CH Instruments with a three electrode system consisting of Ag/AgCl reference electrode, a working electrode and a platinum wire counter-electrode. The redox potentials of the dyes were measured in DCM containing 0.1 M Bu_4NHClO_4 at a scan rate of 100 mV s^{-1}.

2. Synthetic route:

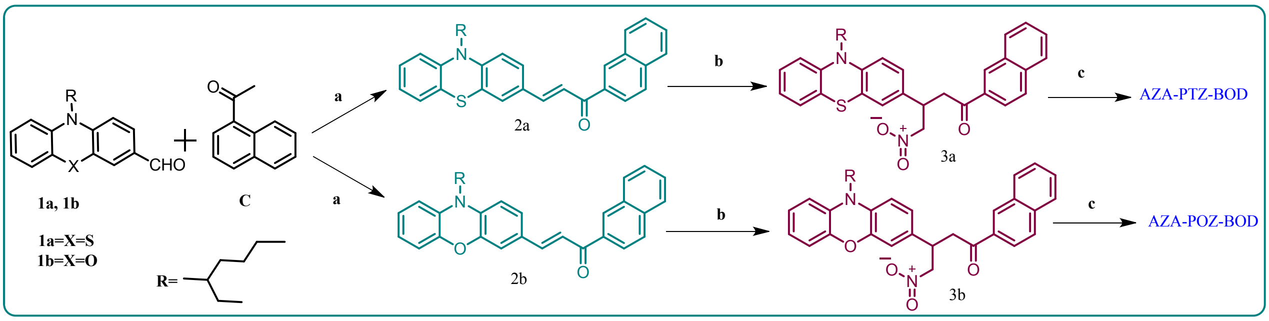

Reagents: a) KOH/Ethanol and H_2O. b) CH_3NO_2, $(CH_3\text{-}CH_2)_2$ NH/Ethanol c) NH_4OAc, DIPEA, BF_3-OEt_2, DCM

The intermediates 1a and 1b was synthesized following previous reports.[1] The intermediates 2a and 2b were synthesized in good yield by the well-known Knoevenagel condensation by the chemical reaction of 1a, 1b, and B intermediates in the presence water and ethanol as solvent and KOH as base. The intermediates 3a and 3b were prepared by Michel addition reaction using nitromethane and diethylamine as base in very good yield. Finally the desired molecules AZA-PTZ-BOD and AZA-POZ-BOD were prepared with ammonium acetate (NH_4OAc), N,N-diisopropylethylamine (DIPEA) and boron trifluoride complex (BF_3-OEt_2) in dichloromethane solution.

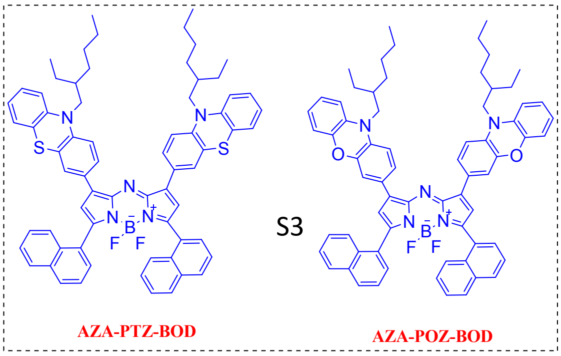

Scheme S1: Preparation of **AZA-PTZ-BOD** and **AZA-POZ-BOD** molecule

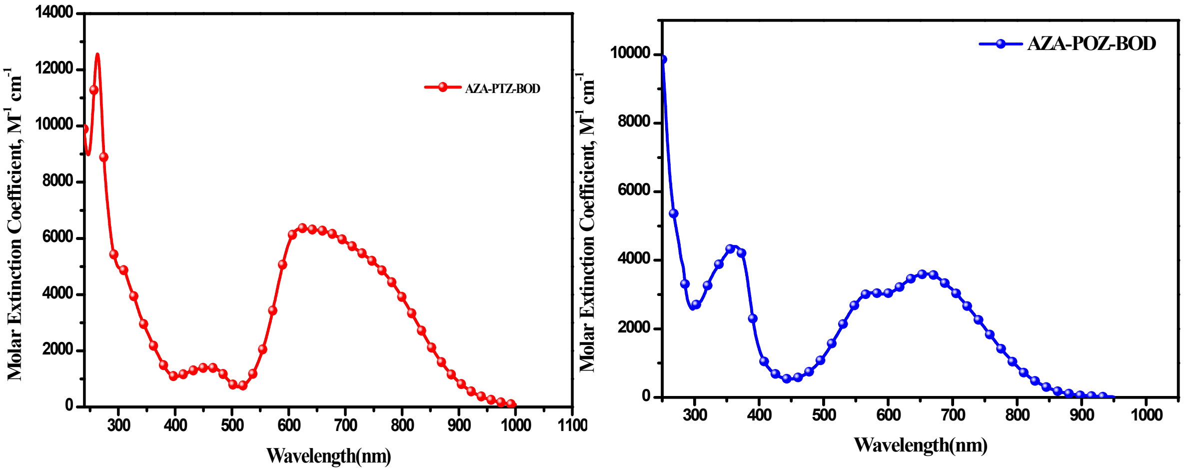

Fig. S1: Molar extinction coefficient spectra of **AZA-PTZ-BOD**and **AZA-POZ-BOD**

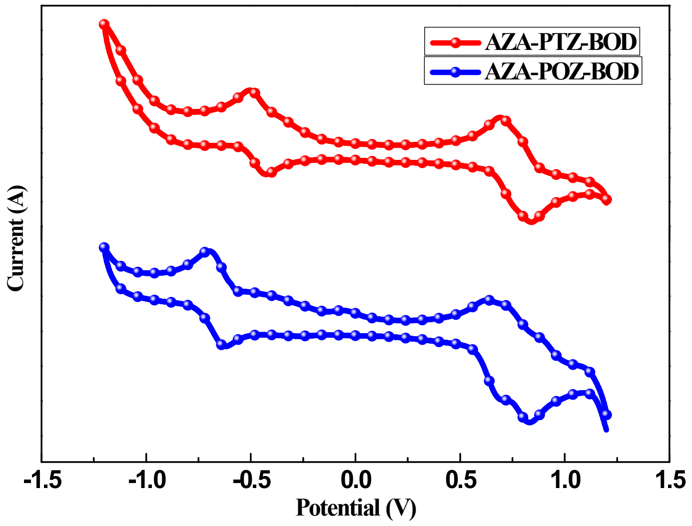

Fig. S2**:** Cyclic voltammogram of dyes in DCM

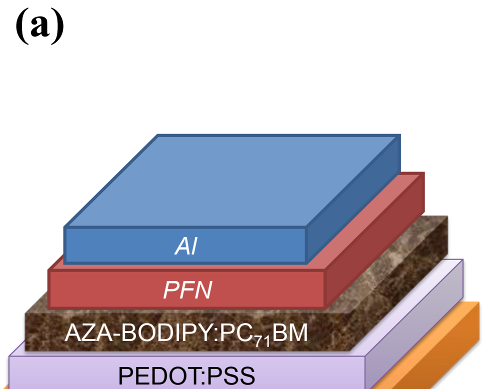

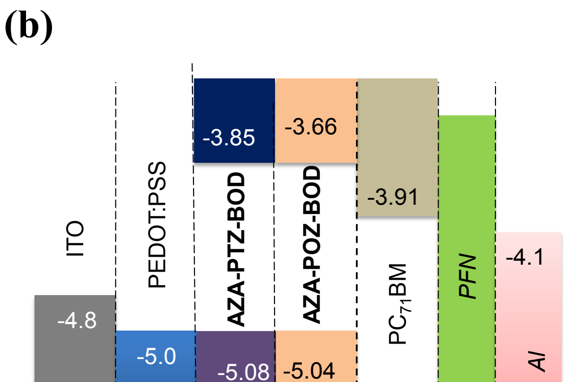

Fig. S3 (a) Energy level diagram of SMs and PC71BM and (b) device structure

6. Device fabrication and characterization:

The organic solar cells were fabricated with a conventional device structure of ITO/PEDOT:PSS/ SMs :$PC_{71}BM$/PFN/Al. The ITO glass substrates were cleaned in ultrasonic bath with detergent, de-ionized water, acetone, and isopropyl alcohol, sequentially and dried in vacuum oven at the temperature of 50 ^{o}C for overnight. A thin layer (about 40 nm) of PEDOT:PSS was then spin coated on the onto the ITO glass at 3500 rpm and annealed at 110 ^{o}C for 20 min. The mixers of AZA-POZ-BOD or AZA-PTZ-BOD/$PC_{71}BM$ in different weight ratios were dissolved in chloroform solution and stirred for overnight and spin coated on top of the PEDOT:PSS layer for form the active BHJ layer of about 85-90 nm and dried in atmospheric environment. For solvent vapor annealing (SVA) treatment, optimized thin films were placed in the petri-disc in the THF environment for 40 s and then dried at room temperature. PFN solution (methanol with some traces of acetic acid) was then spin coated as electron transport layer. Finally, aluminum (Al) electrode was thermally evaporated under $1x10^{-5}$ Pa and device area was 26 mm^2 was defined by a shadow mask. The current -voltage characteristics were measured with a Keithley 2400 source meter unit under stimulated 100 mW/cm^2 irradiation for a solar simulator. The incident photon to current conversion efficiency spectra was recorded using a IPCE measurement unit (Benthem make).

7. Hole and Electron Mobility of Device:

The hole/electron mobilities for as cast active layer are about 7.56 x10^{-5}/2.34 x10^{-4} cm^2/Vs and 8.97x10^{-5}/2.38 x10^{-4} cm^2/ Vs for AZA-PTZ-BOD:PC$_{71}$BM and AZA-POZ-BOD:PC$_{71}$BM with electron to hole mobility ratio of 3.09 and 2.65, respectively, indicating that there is a unbalanced charge transport in the as cast active layer leading to low value of FF in these OPVs. However, both the hole and electron mobility were increased after the SVA treatment and hole/electron mobility's are about 9.86 x10^{-5}/2.45 x10^{-4} cm^2/Vs and 1.24 x10^{-4} /2.52 x10^{-4} cm^2/Vs with electron to hole mobility ratio of 1.97 and 2.48 for AZA-PTZ-BOD:PC$_{71}$BM and AZA-POZ-BOD:PC$_{71}$BM blended films, respectively reduced electron to hole mobility ratio is consistent with the high value of FF for SVA treated OPV Moreover, the high value of FF for AZA-PTZ-BOD:PC$_{71}$BM based OPV as compared to AZA-POZ-BOD:PC$_{71}$BM counterpart may also be attributed to the lowest value of electron to hole mobility ratio, indicating that in AZA-PTZ-BOD:PC$_{71}$BM film the charge transport is more balanced as compared to other devices, resulting the high values of both J_{sc} and FF.[9]

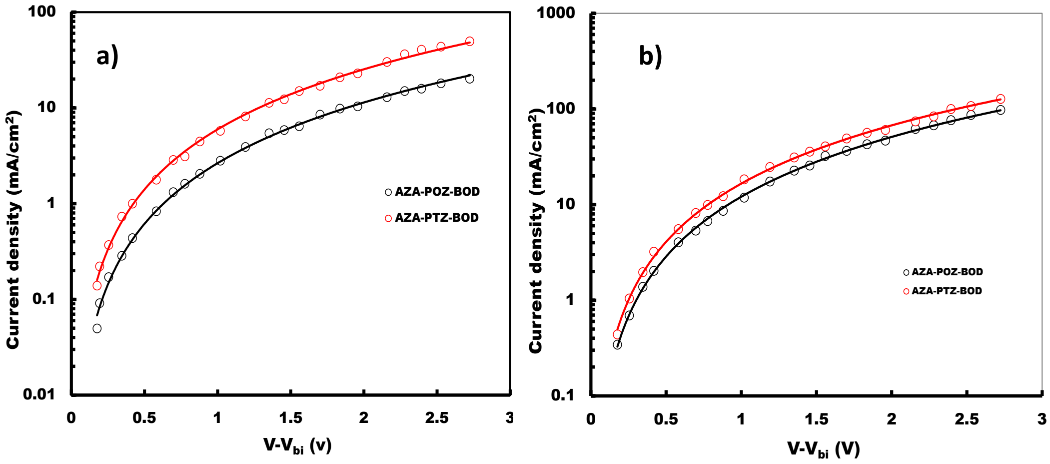

Fig. S4: Dark J-V characteristics of (a) hole only and (b) electron only devices for the optimized active layers (SVA).

8. X-ray diffraction (XRD) Study:

Both the active layer showed two diffraction peaks located at 2θ = 5.04° (same of both active layers) and 2θ = 23.34° and 23.84° for **AZA-POZ-BOD**:$PC_{71}BM$ and **AZA-PTZ-BOD**:$PC_{71}BM$, respectively. The peak at 2θ = 5.04° corresponds to lamellar (100) signal with d-spacing of about 1.78 nm. The peak at 2θ = 23.34° and 23.84° corresponds to π-π stacking (010) with distance of 0.394 nm and 0.373 nm for **AZA-POZ-BOD :** $PC_{71}BM$ and **AZA-PTZ-BOD**:$PC_{71}BM$ active layer respectively. In addition to these peaks, there is a wide peak around 2θ - 18.23° corresponds to the $PC_{71}BM$. It can be seen from XRD pattern that the intensity of the lamellar signal for the active layer based on **AZA-PTZ-BOD** is higher than that for **AZA-POZ-BOD** is an indication of higher crystallinity for former than later. The higher crystallinity and reduced π-π sacking distance is beneficial for the better charge transport and reduced recombination and resulting high values of FF and J_{sc}.

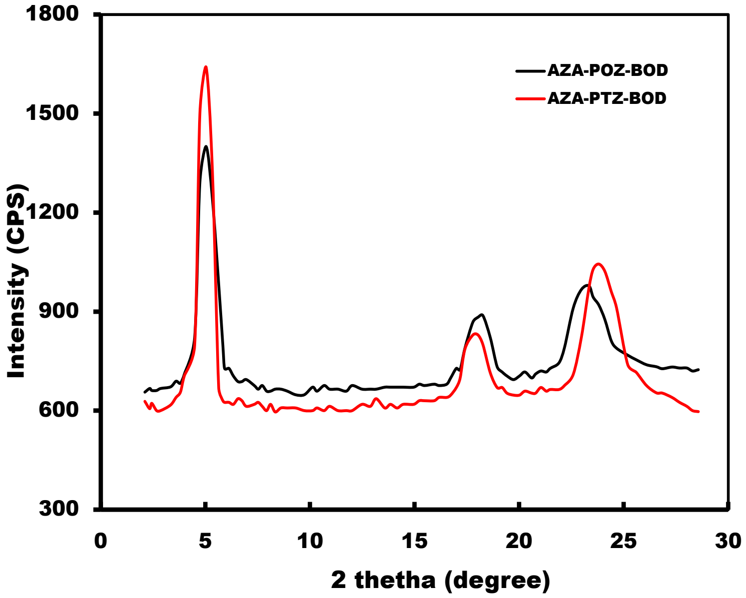

Fig. S5 : X-ray diffraction patterns of the optimized active layers

9. Computational Details of the AZA-BODIPY Dyes.

Density Functional Theory (DFT) and Time-Dependent DFT (TDDFT) calculations were performed using *Gaussian 09* software program package [7]. TDDFT calculations were performed at B3LYP [2] /6-311g (d,p) level of theory in DCM solvent by means of the Polarizable Continuum Model [3,4] (PCM), as implemented in *Gaussian 09*.50 singlet-singlet excitations at S_0 optimized geometry are calculated. The software *GaussSum 2.2.*[5] were used to simulate the major portion of the absorption spectrum and to interpret the nature of transitions. The molecular orbital surfaces are visualized with *Gaussview*, [8] and the molecular orbital were calculated using *GaussSum*.

AZA-POZ-BOD

HOMO 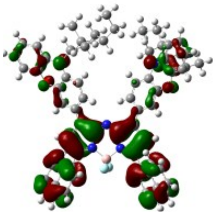	**LUMO** 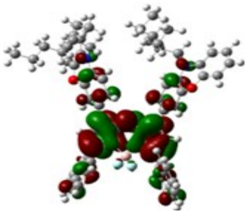
HOMO-1 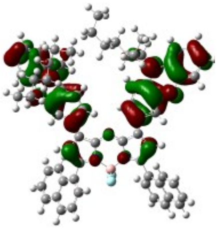	**LUMO+1** 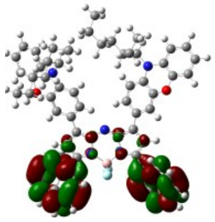
HOMO-2 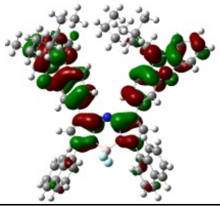	**LUMO+2** 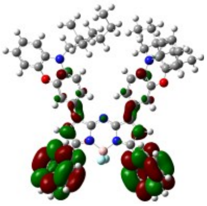
HOMO-3 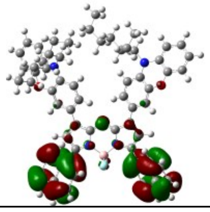	**LUMO+3** 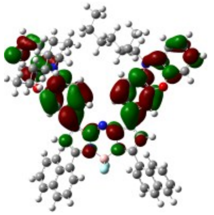

Table S1**:** Molecular orbital of **AZA-POZ-BOD** calculated at B3LYP/6-311g (d,p) level of theory in DCM solvent.

AZA-POZ-BOD				
Excited State	Wavelength (nm)	Osc. Strength	Major contribs	Minor contribs
S1	695.7196	0.7853	HOMO->LUMO (93%)	H-2->LUMO (4%)
S2	571.5664	0.6308	H-1->LUMO (94%)	H-10->LUMO (2%)
S3	522.9194	0.242	H-2->LUMO (90%)	HOMO->LUMO (3%)
S4	394.8541	0.2013	H-3->LUMO (97%)	
S5	373.4801	0.0171	H-6->LUMO (27%), H-4->LUMO (36%)	H-13->LUMO (5%), H-7->LUMO (9%), H-2->LUMO (4%)
S6	362.4209	0.0259	H-6->LUMO (23%), H-4->LUMO (54%)	H-9->LUMO (9%), H-7->LUMO (4%)
S7	357.7155	0.0263	H-10->LUMO (18%), H-5->LUMO (62%)	H-14->LUMO (5%), H-11->LUMO (3%), H-8->LUMO (6%), H-1->LUMO (2%)
S8	330.2898	0.0119	H-17->LUMO (38%), H-6->LUMO (15%)	H-18->LUMO (8%), H-16->LUMO (3%),
S9	320.9614	0.0306	H-10->LUMO (25%), H-8->LUMO (20%), H-5->LUMO (20%)	H-14->LUMO (4%), H-11->LUMO (9%), HOMO->L+3 (5%)
S10	316.133	0.0041	H-17->LUMO (16%), H-7->LUMO (41%), H-6->LUMO (13%)	H-18->LUMO (4%), H-12->LUMO (3%), H-8->LUMO (5%)

Table S2. Major allowed transitions of **AZA-POZ-BOD** calculated at B3LYP/6-311g (d,p)levelof theory in DCM solvent.

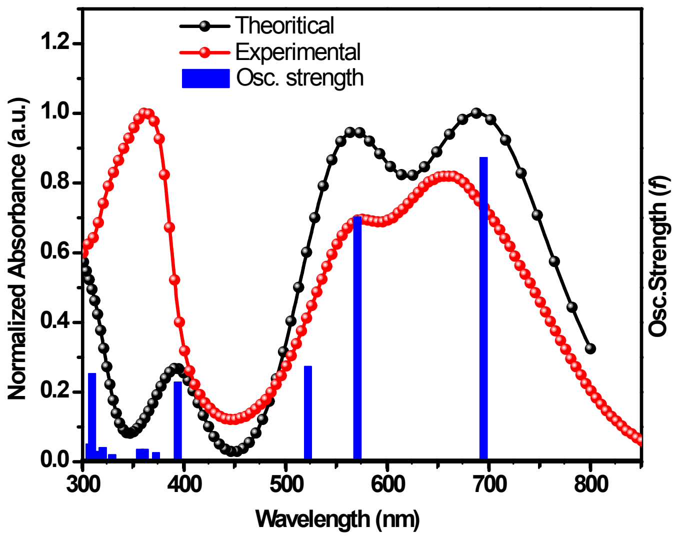

Fig. S6**:** Normalized plots of experimental and simulated absorption spectra of **AZA-POZ-BOD**

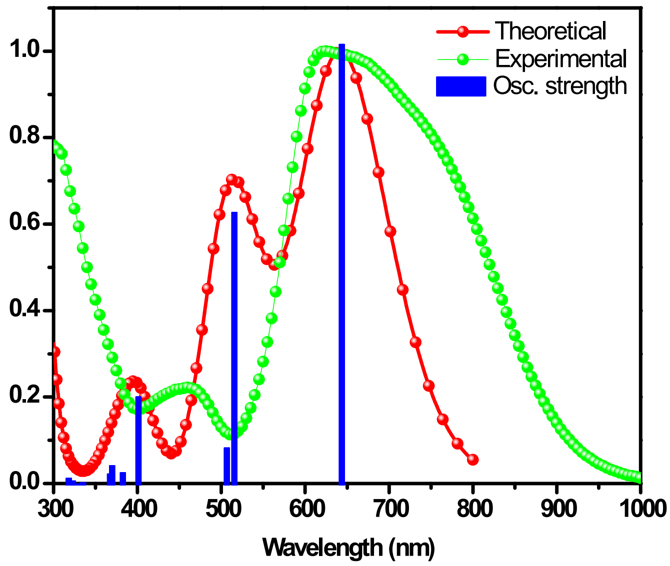

Fig. S7**:** Normalized plots of experimental and simulated absorption spectra of **AZA-PTZ-BOD**

AZA-PTZ-BOD	
HOMO 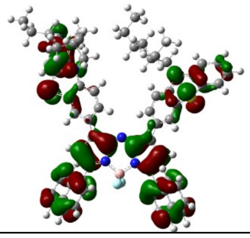	**LUMO** 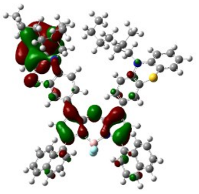
HOMO-1 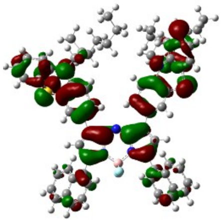	**LUMO+1** 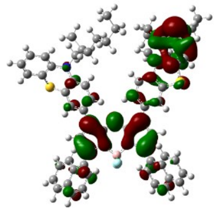
HOMO-2 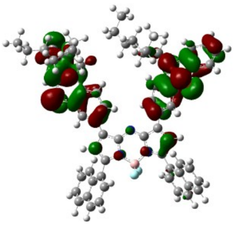	**LUMO+2** 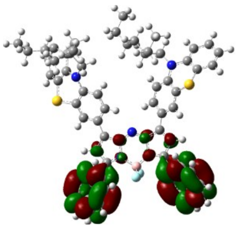
HOMO-3 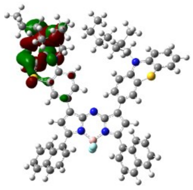	**LUMO+3** 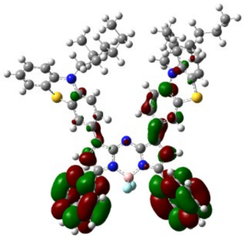

Table S3**:** Molecular orbital of **AZA-PTZ-BOD** calculated at B3LYP/6-311g (d,p) level of theory in DCM solvent.

AZA-PTZ-BOD				
Excited state	Wavelength (nm)	Osc. Strength	Major contribs	Minor contribs
S1	642.2388	0.9525	HOMO->LUMO (92%)	H-2->LUMO (5%)
S2	514.1799	0.5889	H-1->LUMO (91%)	H-8->LUMO (3%)
S3	505.3154	0.0796	H-2->LUMO (84%)	H-7->LUMO (5%), H-4->LUMO (3%),
S4	399.9232	0.1904	H-3->LUMO (96%)	
S5	381.2669	0.0259	H-7->LUMO (12%), H-4->LUMO (63%)	H-13->LUMO (3%), H-8->LUMO (3%), H-2->LUMO (7%)
S6	368.5947	0.0415	H-8->LUMO (13%), H-5->LUMO (68%)	H-14->LUMO (3%), H-11->LUMO (3%), H-9->LUMO (2%), H-1->LUMO (4%)
S7	365.951	0.0235	H-7->LUMO (17%), H-6->LUMO (47%), H-4->LUMO (19%)	H-13->LUMO (2%), H-10->LUMO (3%), H-8->LUMO (4%)
S8	333.7664	0.0049	H-20->LUMO (19%), H-7->LUMO (17%), H-6->LUMO (29%)	H-21->LUMO (8%), H-13->LUMO (5%), H-12->LUMO (6%), H-9->LUMO (2%)
S9	327.4115	0.0017	H-8->LUMO (51%), H-5->LUMO (18%)	H-14->LUMO (7%), H-11->LUMO (5%), H-9->LUMO (2%), H-6->LUMO (3%)
S10	321.5691	0.0083	H-21->LUMO (10%), H-20->LUMO (32%), H-7->LUMO (24%)	H-16->LUMO (2%), H-10->LUMO (4%), H-6->LUMO (8%), H-4->LUMO (5%)

Table S4. Major allowed transitions of **AZA-PTZ-BOD** calculated at B3LYP/6-311g (d,p)level of theory in DCM solvent.

10. Experimental Section

Synthesis:

10-(2-ethylhexyl)-10*H*-phenothiazine-3-carbaldehyde(1a),10-(2-ethylhexyl)-10*H* phenoxazine-3-carbaldehyde (1b), 1-(napthalen-1-yl) ethanone (B) was synthesized according to literature procedure[6].

(*E*)-3-(10-(2-ethylhexyl)-10*H*-phenothiazin-2-yl)-1-(naphthalen-2-yl)prop-2-en-1-one (2a):

To a stirred solution of compound **1a** (4g, 9.4 mmol), KOH (2.28g ,56 mmol) in water 20 ml and ethanol 70 ml, compound **B** (2.44g, 14.34 mmol) in ethanol (25 mL) was added drop wise. The reaction mixture was stirred for 6 h at room temperature. The solid was filtrated and carefully washed to neutral with cold water. The crude product was purified by column chromatography (eluent: EtOAc/hexane 1:4) to furnish **2a** (3.923g, 85%) as a yellowish liquid.**^{1}H NMR (300 MHz, CDCl$_3$)**: δ (ppm) = 8.30 - 8.27 (m, 1H), 7.99 (d, *J* = 8.2 Hz, 1H), 7.92 - 7.89 (m, 1H), 7.72 (d, *J* = 8.0 Hz, 1H), 7.56 - 7.52 (m, 3H), 7.40 (d, *J* = 15.9 Hz, 1H), 7.06 (d, *J* = 15.8 Hz, 1H), 6.95 (dd, *J* = 8.4, 1.8 Hz, 1H), 6.87 (s, 1H), 6.82 - 6.76 (m, 1H), 6.71 - 6.61 (m, 2H), 6.55 (d, *J* = 7.9 Hz, 1H), 6.48 (d, *J* = 8.4 Hz, 1H), 3.44 (d, *J* = 7.2 Hz, 2H), 1.90 - 1.83 (m, 1H), 1.38 - 1.25 (m, 8H), 0.95 - 0.86 (m, 6H). **^{13}C NMR (101 MHz, CDCl$_3$)**: δ (ppm) 195.7, 145.3, 145.2, 144.7, 137.7, 136.9, 133.8, 132.6, 131.1, 130.5, 128.4, 127.2, 126.7, 126.4, 125.7, 124.5, 124.1, 123.6, 121.8, 115.7, 113.6, 112.5, 111.7, 47.7, 36.7, 30.74, 29.7, 28.8, 24.1, 23.1, 14.0, 11.0. HRMS [M + H]+ (*m/z*):calcd.for$C_{33}H_{33}NOS$, [M + H]$^+$ m/z 491.68, found 492.23.

3-(10-(2-ethylhexyl)-10*H*-phenothiazin-2-yl)-1-(naphthalen-1-yl)-4-nitrobutan-1one (3a):

A mixture of a compound **2a** (3.80 g, 7.73 mmol), nitromethane (2.35g, 38.61 mmol) and diethylamine (2.817g 38.6 mmol) dissolved in ethanol (100 mL) was heated to reflux for 6-12 h. After cooling at room temperature, the solvent was removed in vacuum and the oily residue obtained was dissolved in ethyl acetate and washed with water. The combined organic layers were washed with brine solution, dried over sodium sulphate, and concentrated. Further purification by column chromatography on silica eluting with CH_2Cl_2/hexane (1:1) and evaporation of the solvent gave the target compound as colourless oily residue (2.90 g, 68%).**^{1}H NMR (300 MHz, $CDCl_3$)**: δ(ppm) 8.44 (d, *J* = 7.6 Hz, 1H), 7.99 (d, *J* = 8.2 Hz, 1H), 7.83 (dd, *J*= 15.3, 6.8 Hz, 2H), 7.58 - 7.45 (m, 3H), 6.76 (t, *J* = 8.4 Hz, 1H), 6.67 - 6.56 (m, 3H), 6.50 (d, *J* = 9.7 Hz, 2H), 6.39 (d, *J* = 8.3 Hz, 1H), 4.79 - 4.73 (m, 1H), 4.67 - 4.60 (m, 1H), 4.10 - 4.06 (m, 1H), 3.44 (d, *J* = 7.1 Hz, 2H), 3.34 (d, *J* = 7.3 Hz, 2H), 1.82 - 1.80 (m, 1H), 1.40 - 1.25 (m, 8H), 0.88 (m, *J* = 8H).**^{13}C NMR (101 MHz, $CDCl_3$)**:δ (ppm) 201.0 , 145.3 , 144.7 , 135.3 , 133.9 (d, *J* = 10.9 Hz), 133.1 , 131.0 , 130.0 , 128.4 , 128.1 , 127.6 , 126.6 , 125.6 , 124.3 , 123.6 , 122.7 , 120.9 , 115.4 , 114.2 , 112.0, 79.6, 47.8, 44.7, 39.0, 36.6, 30.7, 28.8, 24.1, 23.1, 14.0, 11.0. **HRMS (ESI)** m/z calcd. for $C_{34}H_{36}N_2O_3SNa$: m/z $[M+Na]^+$ 552.72, found 553.25.

1,9-bis(10-(2-ethylhexyl)-10*H*-phenothiazin-2-yl)-5,5-difluoro-3,7-di(naphthalen-1-yl)-5*H*-dipyrrolo[1,2-c:2',1'-f][1,3,5,2]triazaborinin-4-ium-5-uide (AZA-PTZ-BOD):

A 500 mL round-bottomed flask was charged with compound **3a** (2.80 g, 5.07 mmol) and ammonium acetate (20.20 g, 200 mmol), and *t*-butanol 80 ml the mixture was heated at 130 ^oC for 12 h. The reaction mixture in the round-bottomed flask was allowed to cool to room temperature. Then CH_2Cl_2 (200 mL) and water (50mL) was added. The organic layer was separated, washed with water (3×50 mL) and dried over sodium sulphate. The solvent was evaporated to give the product as a dark blue solid which was used in the next step without further purification. The crude product was dissolved in dry CH_2Cl_2 (80 mL), treated with diisopropyl ethyl amine (1.3 mL, 10.12 mmol) and boron tri-fluoride diethyletherate (1.5mL, 12.68 mmol), and stirred at room temperature under N_2 for 24 h. The mixture was washed with water (50 mL), and organic layer was dried over sodium sulphate and evaporated to dryness. Purification by column chromatography on silica eluting with CH_2Cl_2/hexane (2:3) and evaporation of the solvent gave the product green amorphous solid (0.16 g, 30%). **^{1}H NMR (400 MHz, CDCl$_3$)**: *δ* (ppm)= 8.04 (d, *J* = 2.0 Hz, 1H), 8.02 (d, *J* = 2.0 Hz, 1H), 7.98 (dd, *J* = 9.7, 2.7 Hz, 4H), 7.88 - 7.81 (m, 6H), 7.44 (t, *J* = 8.2 Hz, 6H), 7.21- 7.15 (m, 4H), 7.09 (d, *J* = 8.6 Hz, 2H), 6.97-6.93 (m, 4H), 6.82 (s, 2H), 3.86 (d, *J* = 8.6 Hz, 4H), 2.06 - 2.00 (m, 2H), 1.43 - 1.25 (m, 16H), 0.91 (t, *J* = 7.4 Hz, 6H), 0.86 (t, *J* = 7.1 Hz, 6H**). ^{13}C NMR (126 MHz, CDCl$_3$)**: δ (ppm) = 157.9, 147.3 , 145.1, 144.6, 142.0, 133.5, 131.5, 130.2, 129.6, 129.0, 28.0, 127.6, 127.3, 126.7, 126.0, 125.3, 124.9, 122.9, 118.9, 116.2, 51.3, 36.0, 30.7, 28.5, 23.9, 23.1, 14.0, 10.5. **MALDI- TOF** m/z calcd. for $C_{69}H_{66}BF_2N_5S_2$ m/z [M+H]+ 1063.466, found 1063.60

(*E*)-3-(10-(2-ethylhexyl)-10*H*-phenoxazin-2-yl)-1-(naphthalen-2-yl)prop-2-en-1-one (2b):

Followed similar procedure as 2a: **1b** (4g, 12.3 mmol), **B** (3.15g, 18.54 mmol), gave **POZ-NAP** (4.200 g, 71%) as a yellowish liquid gel.**^{1}H NMR (300 MHz, CDCl$_3$)** : δ (ppm) = 8.28 (d, J = 9.5 Hz, 1H), 7.97 (d, J = 8.2 Hz, 1H), 7.90 (d, J = 9.4 Hz, 1H), 7.72 (d, J = 7.8 Hz, 1H), 7.53 (dd, J = 12.2, 4.7 Hz, 3H), 7.40 (d, J = 15.8 Hz, 1H), 7.06 (d, J = 15.8 Hz, 1H), 6.94 (d, J = 8.3 Hz, 1H), 6.87 (s, 1H), 6.79 (t, J = 8.3 Hz, 1H), 6.71-6.62 (m, 2H), 6.56-6.46 (m, J = 2H), 3.44 (d, J = 5.1 Hz, 2H), 1.89-1.83 (m,1H), 1.50-1.28 (m, 8H), 0.94 – 0.87 (m, 6H). **^{13}C NMR (126 MHz, CDCl$_3$) :**δ (ppm) = 145.35, 145.14, 144.76, 137.73, 136.90, 133.85, 132.65, 131.20, 130.55, 128.41, 127.28, 126.77, 126.45, 125.80, 124.59, 124.10, 123.67, 121.88, 115.69, 113.67, 112.51, 111.75, 47.73, 36.72, 30.74, 29.75, 28.80, 24.15, 23.12, 14.08, 11.02.**HRMS (ESI)** m/z calcd. for $C_{33}H_{33}NO_2$, $[M + H]^+$ m/z 475.20, found 475.25

3-(10-(2-ethylhexyl)-10*H*-phenoxazin-2-yl)-1-(naphthalen-1-yl)-4-nitrobutan-1-one (3b):

Followed similar procedure as 2a: **2b** (4.00 g, 8.14 mmol), nitromethane (2.44 g,40.70 mmol), and diethylamine (3.02g 41.50 mmol) yielded colourless oily residue yield (2.92 g, 65%). **^{1}H NMR (300 MHz, CDCl$_3$)** : δ (ppm) = 8.44 (d, *J* = 8.9 Hz, 1H), 7.99 (d, *J* = 8.2 Hz, 1H), 7.87 - 7.80 (m, 2H), 7.57 - 7.45 (m, 3H), 6.79 - 6.74 (m, 1H), 6.67 - 6.63 (m, 3H), 6.50 (t, *J* = 4.8 Hz, 2H), 6.39 (d, *J* = 8.3 Hz, 1H), 4.79 - 4.73 (m, 1H), 4.67 - 4.61 (m, 1H), 4.11 -

4.06 (m, 1H), 3.45 (d, *J* = 7.1 Hz, 2H), 3.34 (d, *J* = 7.3 Hz, 2H), 1.89 -1.75 (m, 1H), 1.41-1.25 (m, 8H), 0.92-0.85(m, 6H).**^{13}C NMR (126 MHz, CDCl$_3$)** δ (ppm) = 201.0, 145.3, 144.7, 135.3, 133.9, 133.1, 131.0, 130.0, 128.4, 128.1, 127.6, 126.6, 125.6, 124.3, 123.6, 122.7, 120.9, 115.4, 114.2, 112.0, 79.6, 47.8, 44.7, 39.0, 36.6, 30.7, 28.8, 24.1, 23.1, 14.0, 11.0.**HRMS (ESI)** m/z calcd. for $C_{34}H_{36}N_2O_4Na[M+Na]^+$m/z 536.26, found 536.26.

1,9-bis(10-(2-ethylhexyl)-10*H*-phenoxazin-2-yl)-5,5-difluoro-3,7-di(naphthalen-1-yl)-5*H*-dipyrrolo[1,2-c:2',1'-f][1,3,5,2]triazaborinin-4-ium-5-uide (AZA-POZ-BOD):

Similar procedure followed as **AZA-PTZ-BOD** compound **3a** (2.80 g, 5.22 mmol) and ammonium acetate (8.03g, 20 mmol), and *t*-butanol 80 ml the mixture was heated at 130 °C for 12 h. The product blue amorphous solid (0.17 g, 32%).**^{1}H NMR (300 MHz, CDCl$_3$)**: δ (ppm) = 8.77 (d, J = 8.5 Hz, 1H), 7.88 (d, J = 7.8 Hz, 3H), 7.72 (d, J = 8.3 Hz, 1H), 7.52-7.47 (m, 3H), 7.40-7.37 (m, 1H), 7.05 (s, 1H), 6.77 (t, J = 7.5 Hz, 1H), 6.67 – 6.59 (m, 3H), 6.55 (d, J = 7.9 Hz, 1H), 3.46 (d, J = 6.3 Hz, 2H), 1.95 -1.88 (m, 1H), 1.37-1.28 (m, 8H), 0.92 - 0.86 (m, 6H). **^{13}C NMR (126 MHz, CDCl$_3$)**: δ (ppm) 201.04, 145.34, 144.76, 135.33, 133.92, 133.15, 131.02, 130.04, 128.46, 128.13, 127.64, 126.62 , 125.62, 124.32, 123.61, 122.72, 120.91, 115.48 , 114.21, 112.09, 79.65 , 47.87, 44.70, 39.00, 36.68, 30.77, 28.82, 24.17, 23.14, 14.08, 11.01.MALDI-TOF calcd.for $C_{69}H_{66}BF_2N_5O_2$ m/z $[M+H]^+$ 1031.466, found 1031.78

11. Copies of ^{1}H-NMR and ^{13}C-NMR Spectra:

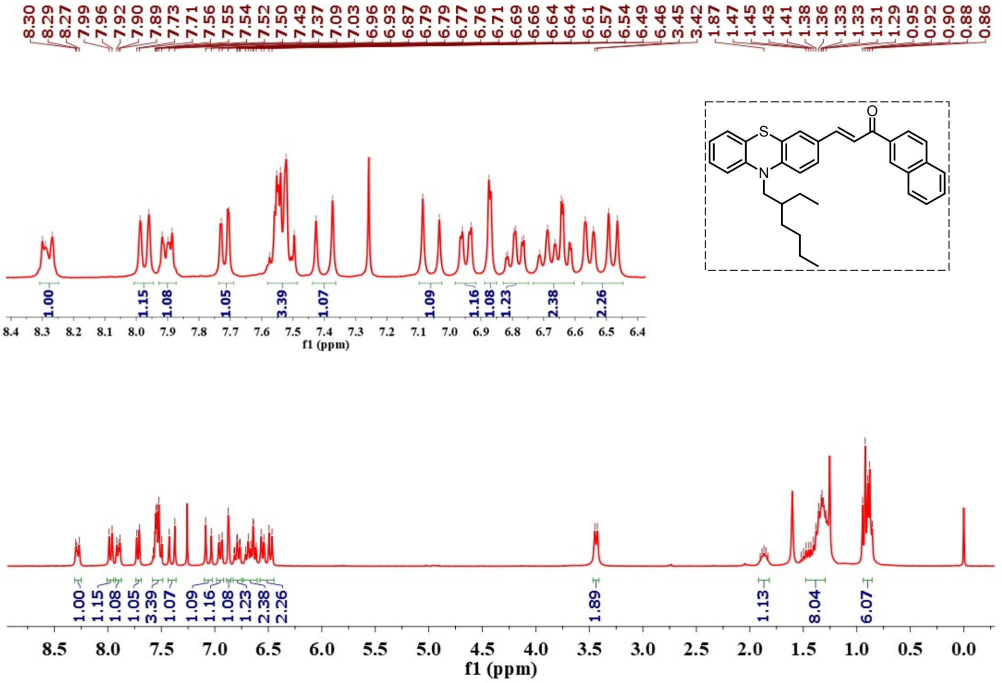

Fig.S8: ^{1}HNMR Spectra of **2a** recorded in $CDCl_3$

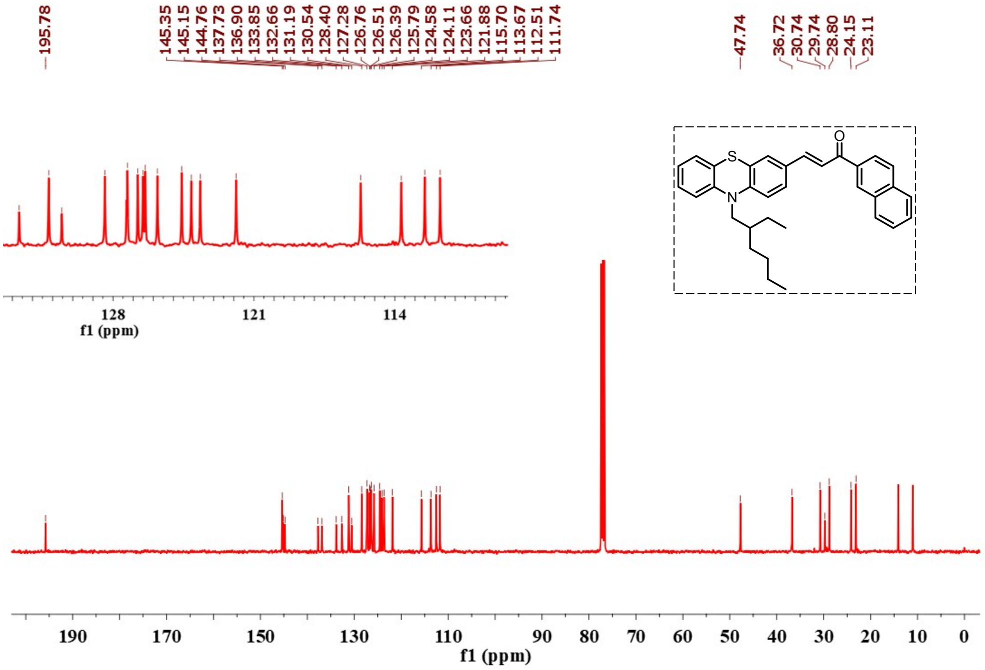

Fig.S9**:** ^{13}CNMR Spectra of **2a** recorded in CDCl$_3$

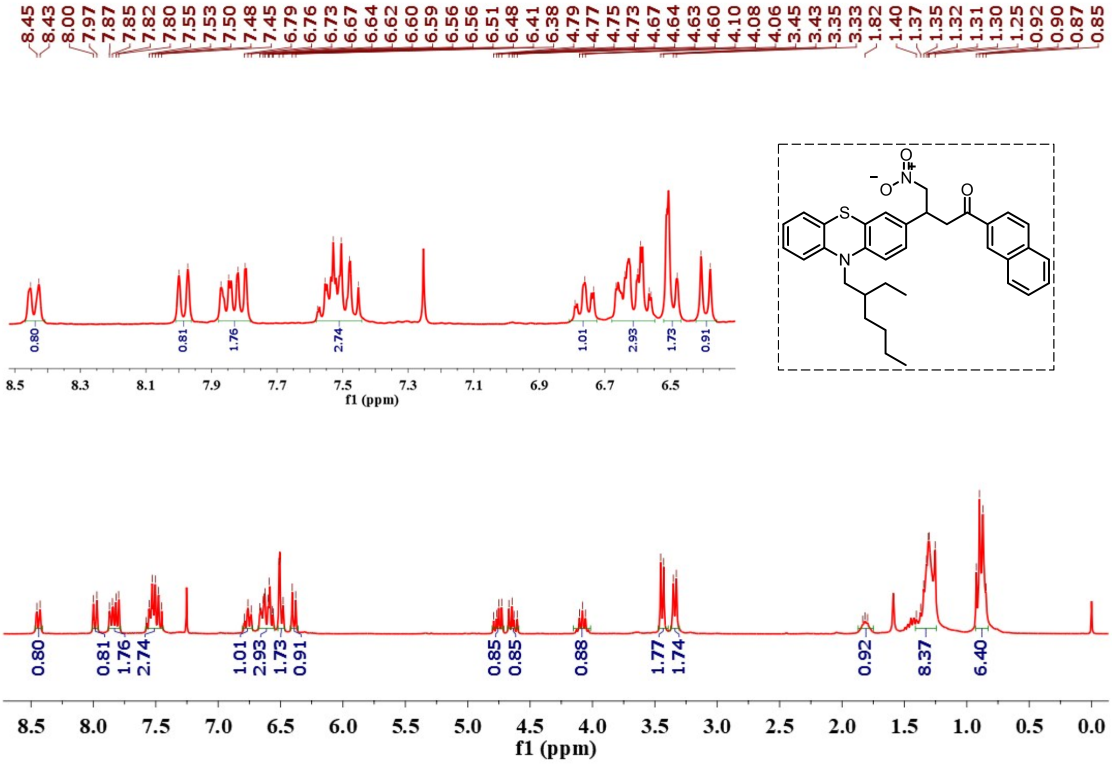

Fig.S10**:** ^{1}HNMR Spectra of **2b** recorded in CDCl$_3$

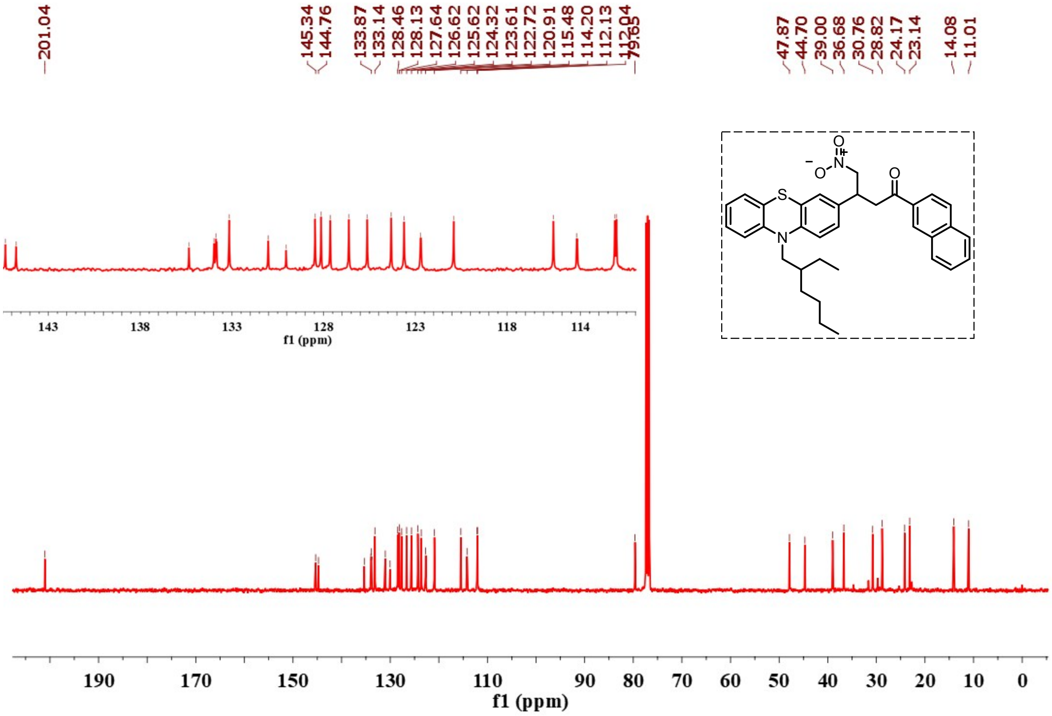

Fig.S11**:** ^{13}CNMR Spectra of **2b** recorded in CDCl$_3$

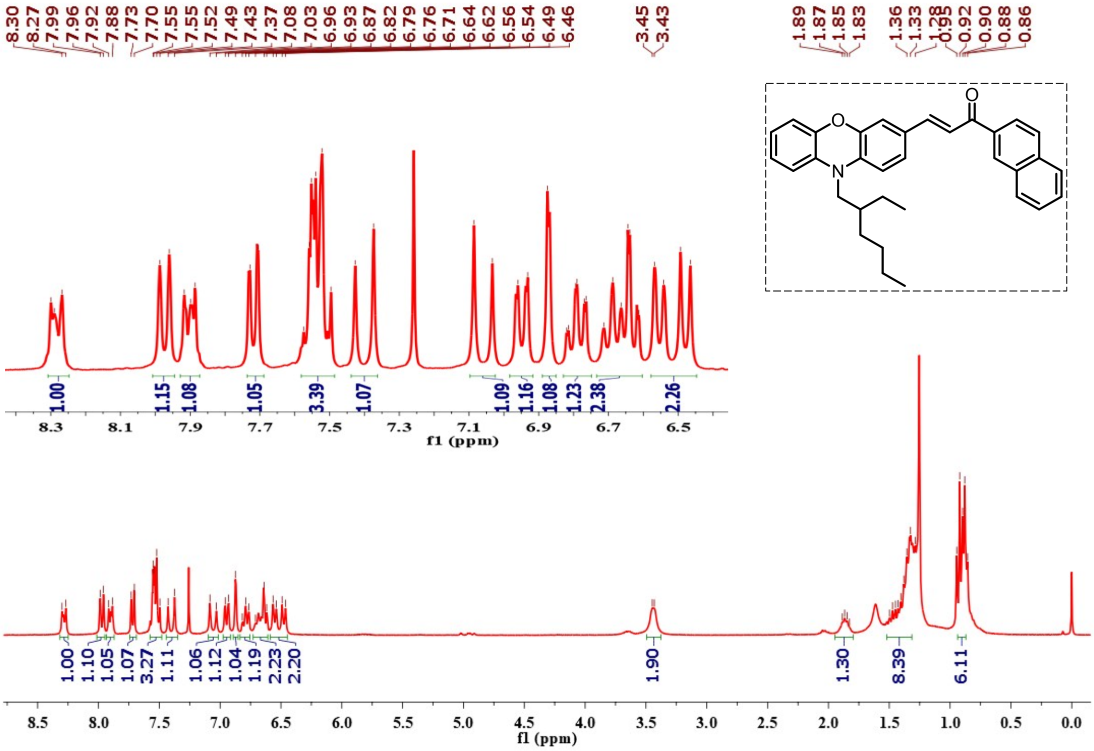

Fig.S12: ^{1}HNMR Spectra of **3a** recorded in $CDCl_3$

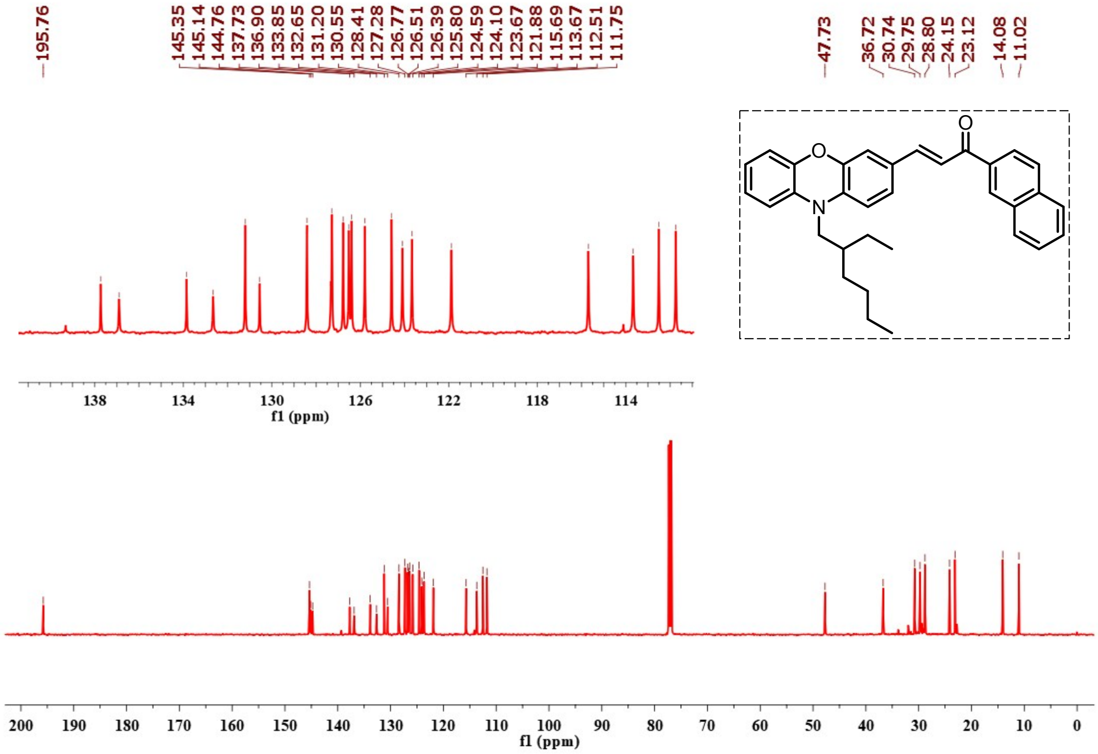

Fig. S13: ^{13}CNMR Spectra of **3a** recorded in CDCl$_3$

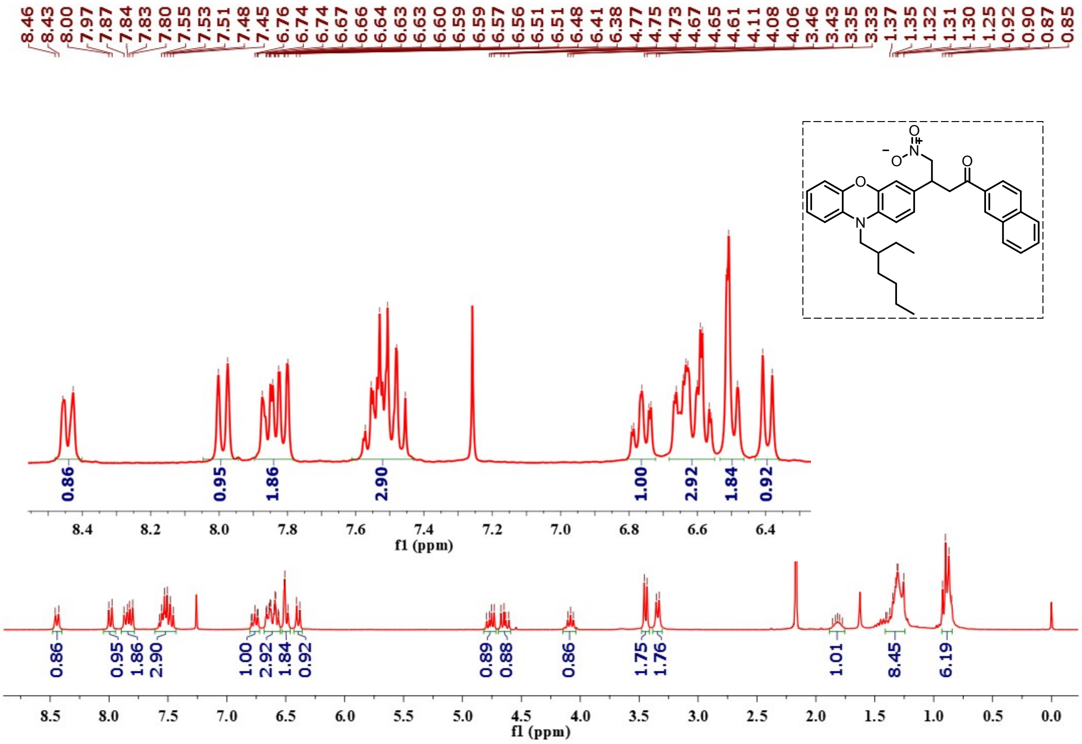

Fig. S14: ^{1}HNMR Spectra of **3b** recorded in CDCl$_3$

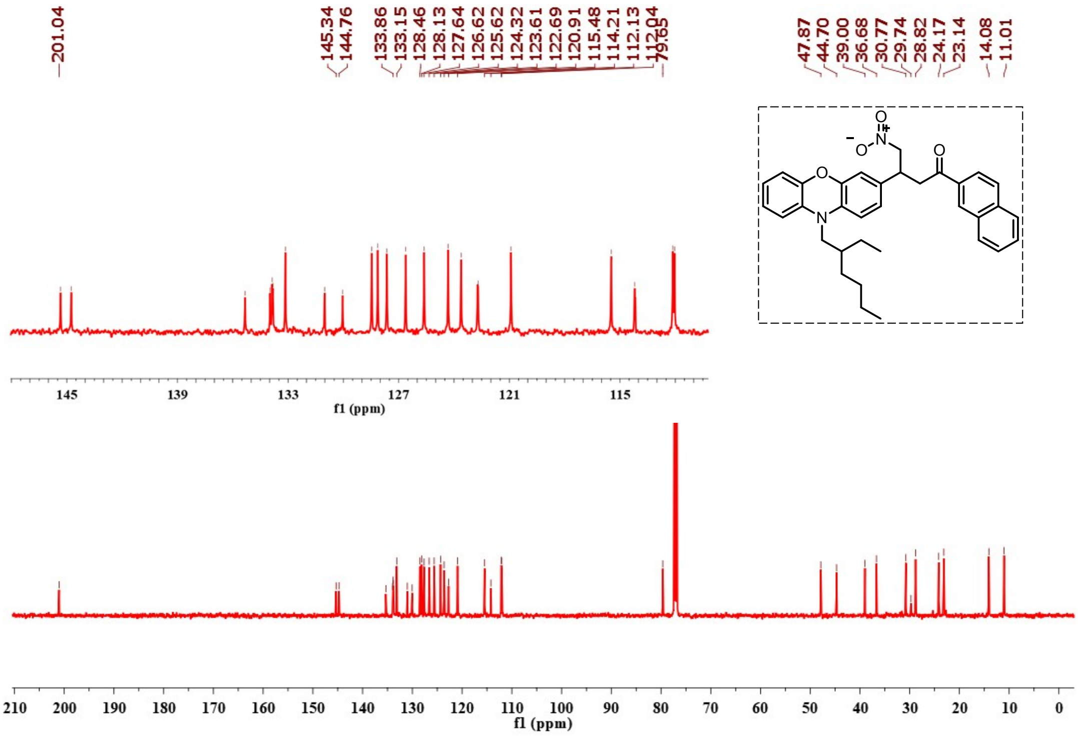

Fig. S15**:** ^{13}CNMR Spectra of **3b** recorded in CDCl$_3$

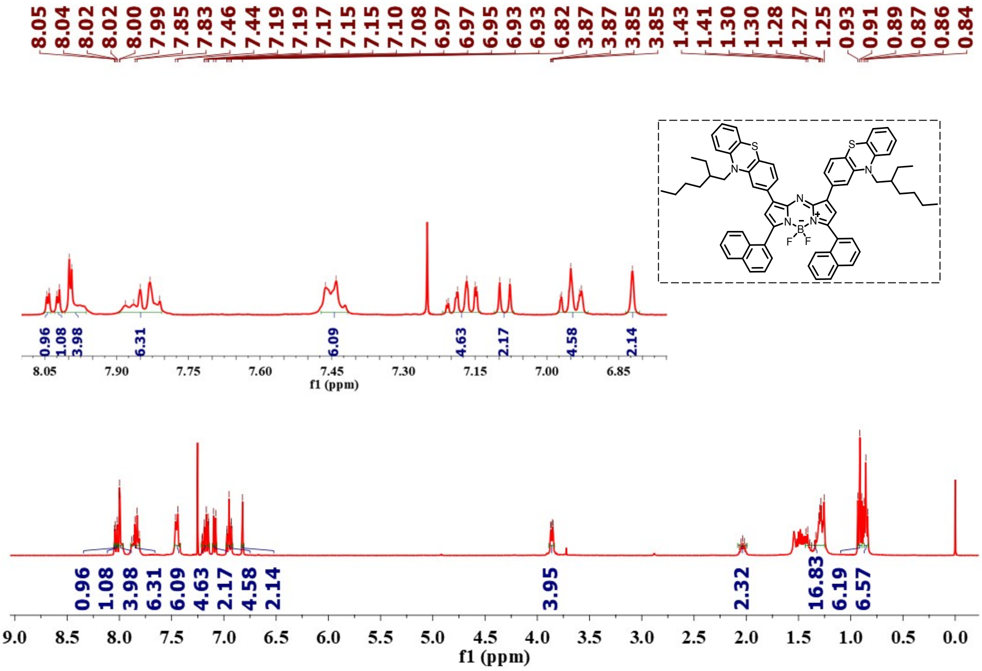

Fig. S16**:** ^{1}HNMR Spectra of **AZA-PTZ-BOD** recorded in CDCl$_3$

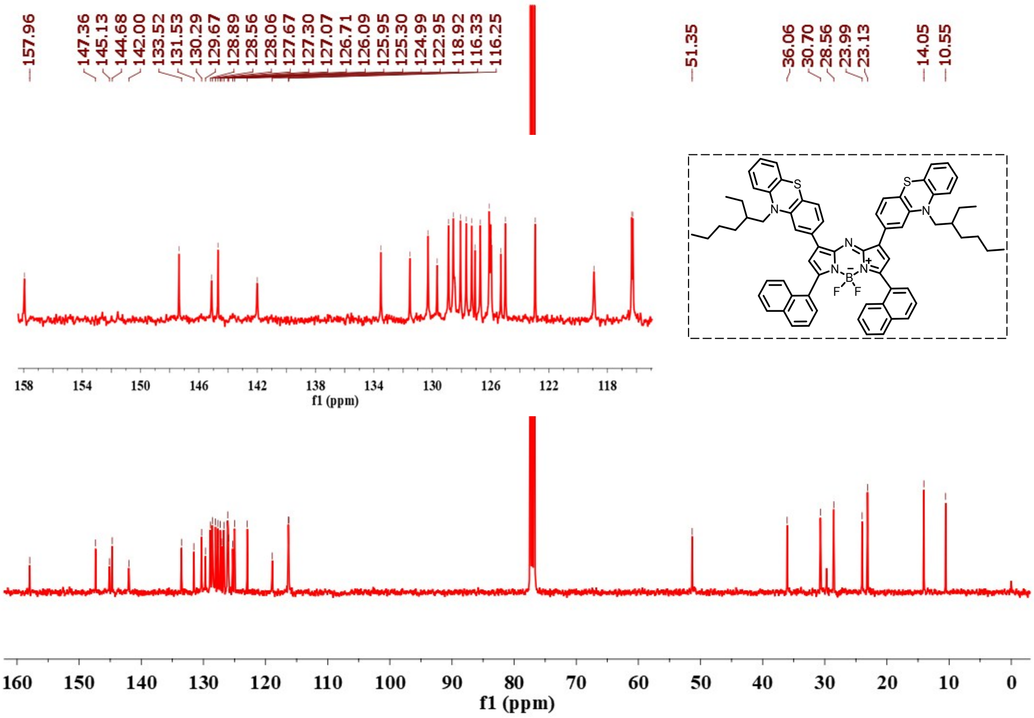

Fig. S17: ^{13}CNMR Spectra of **AZA-PTZ-BOD** recorded in $CDCl_3$

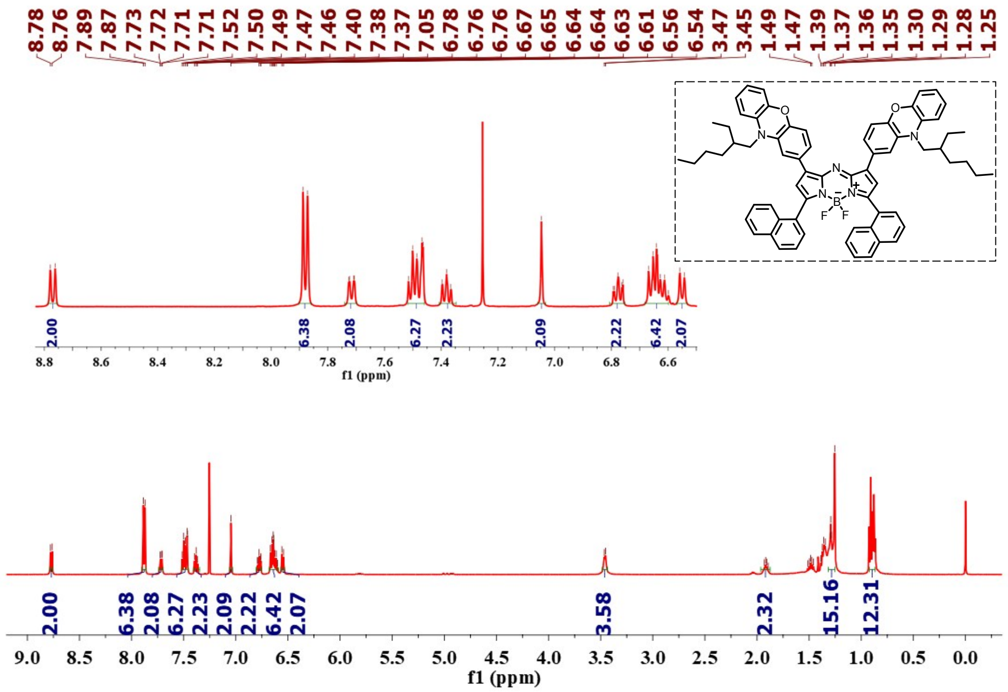

Fig. S18: ^{1}HNMR Spectra of **AZA-POZ-BOD** recorded in $CDCl_3$

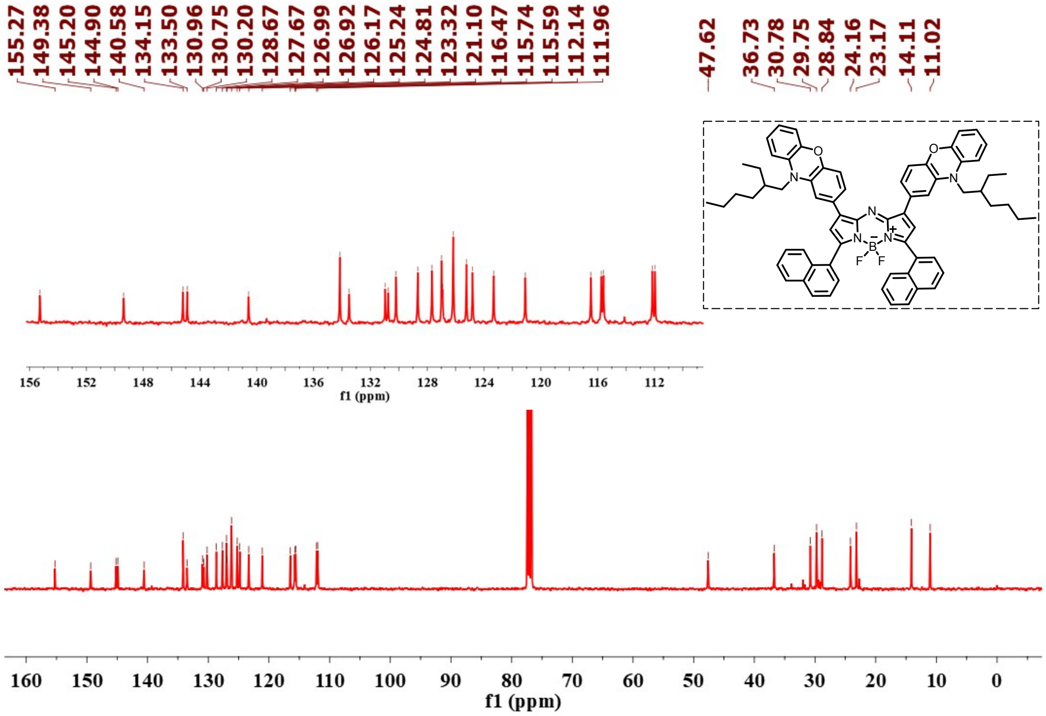

Fig. S19**:** ^{13}CNMR Spectra of **AZA-POZ-BOD** recorded in $CDCl_3$

12. **Copies of HRMS and MALDI-TOF**

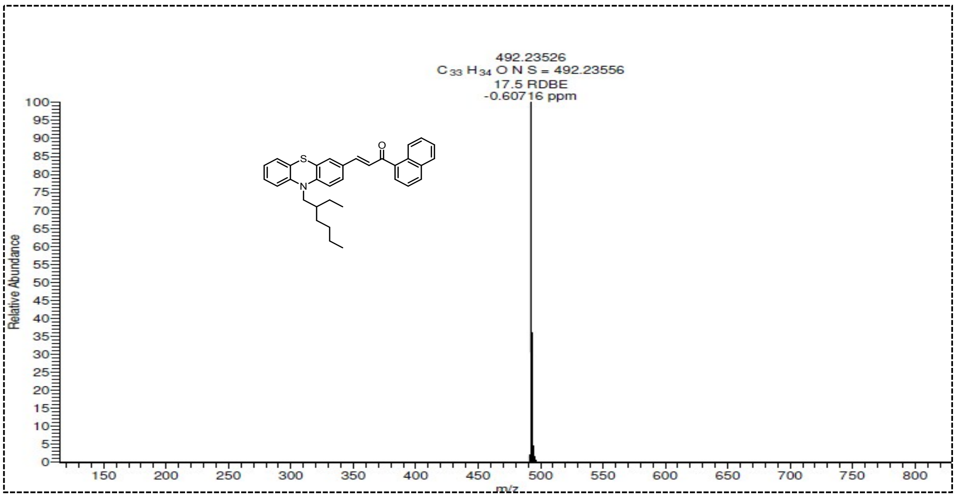

Fig. S20**:** HRMS spectrum of **2a**

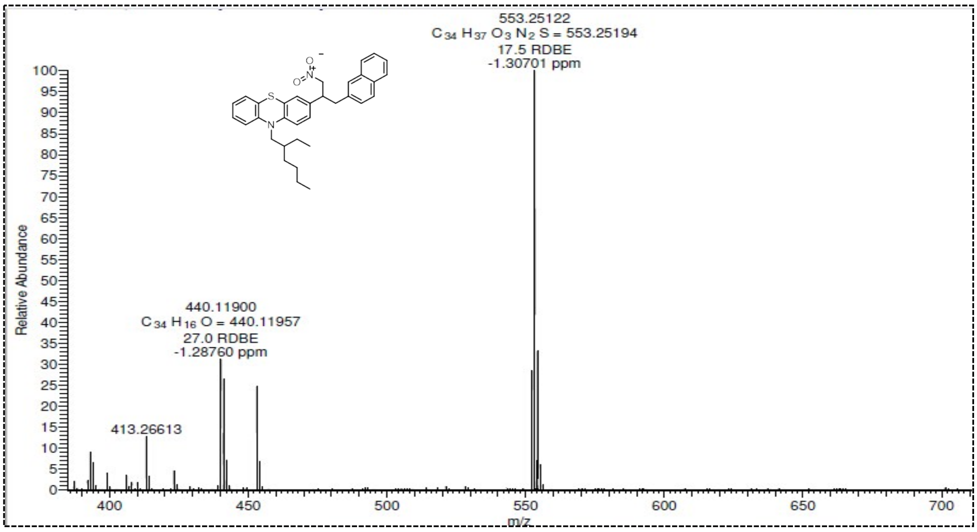

Fig. S21**:** HRMS spectrum of **2b**

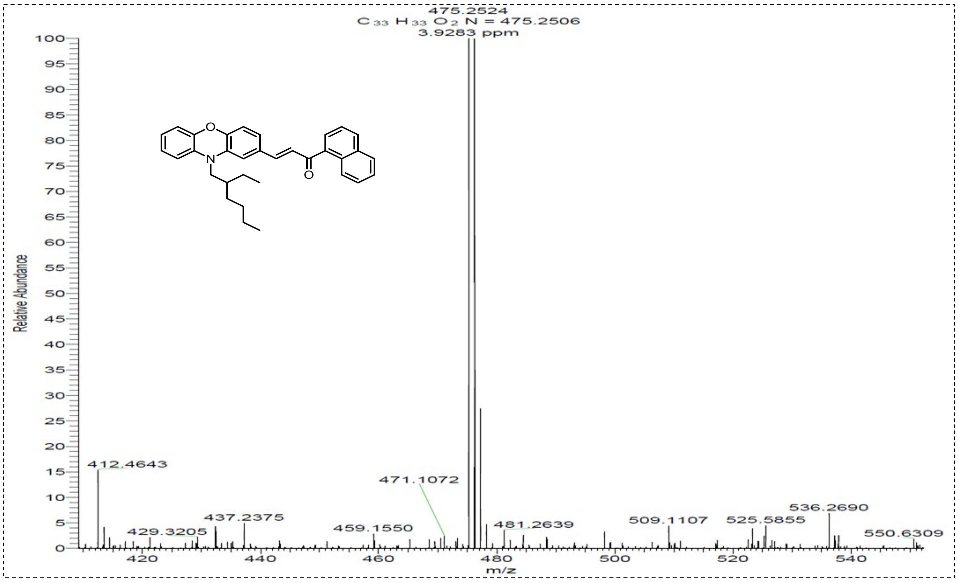

Fig. S22**:** HRMS spectrum of **3a**

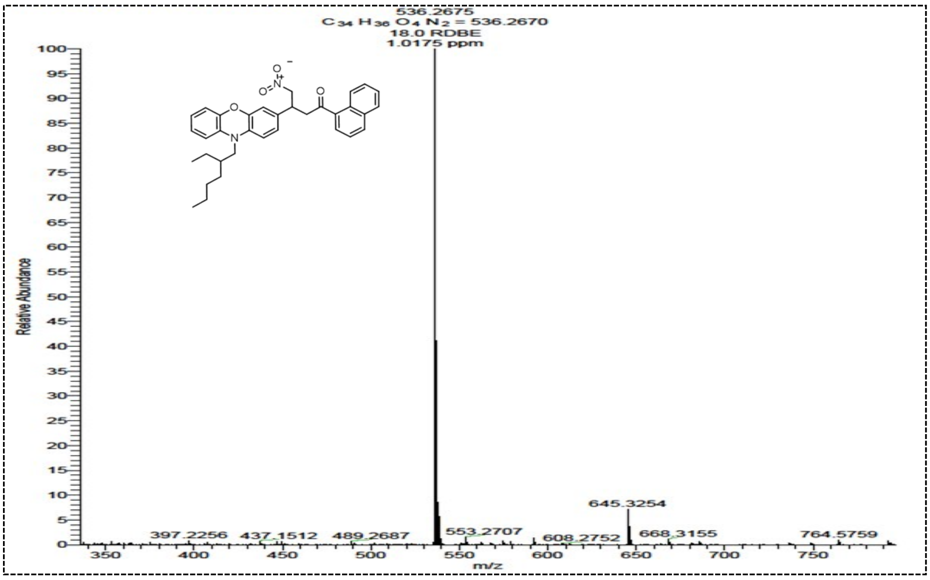

Fig. S23**:** HRMS spectrum of **3b**

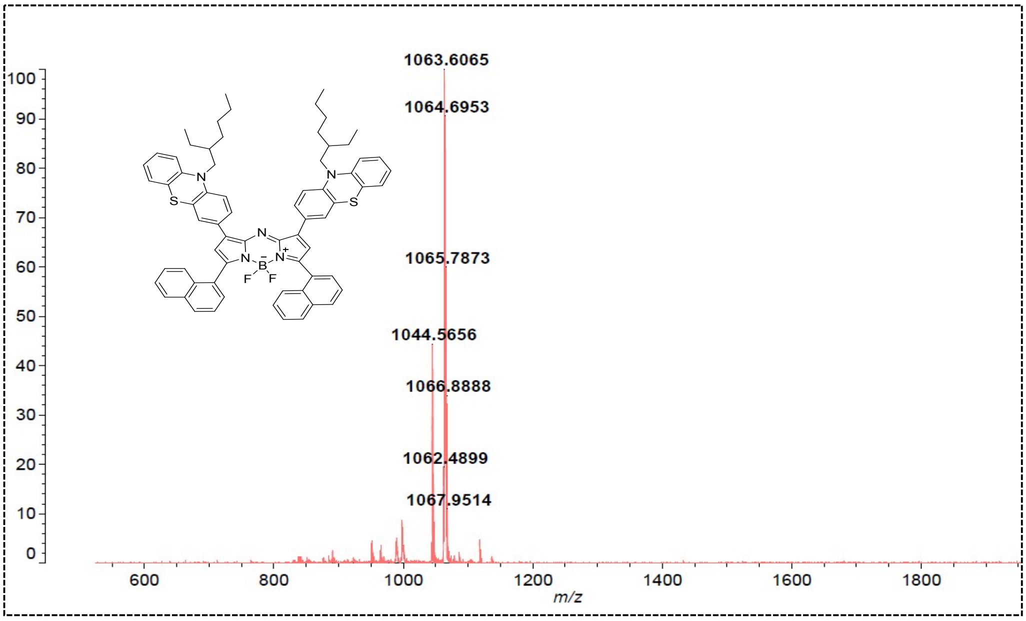

Fig. S24**:** MALDI-TOF spectrum of **AZA-PTZ-BOD**

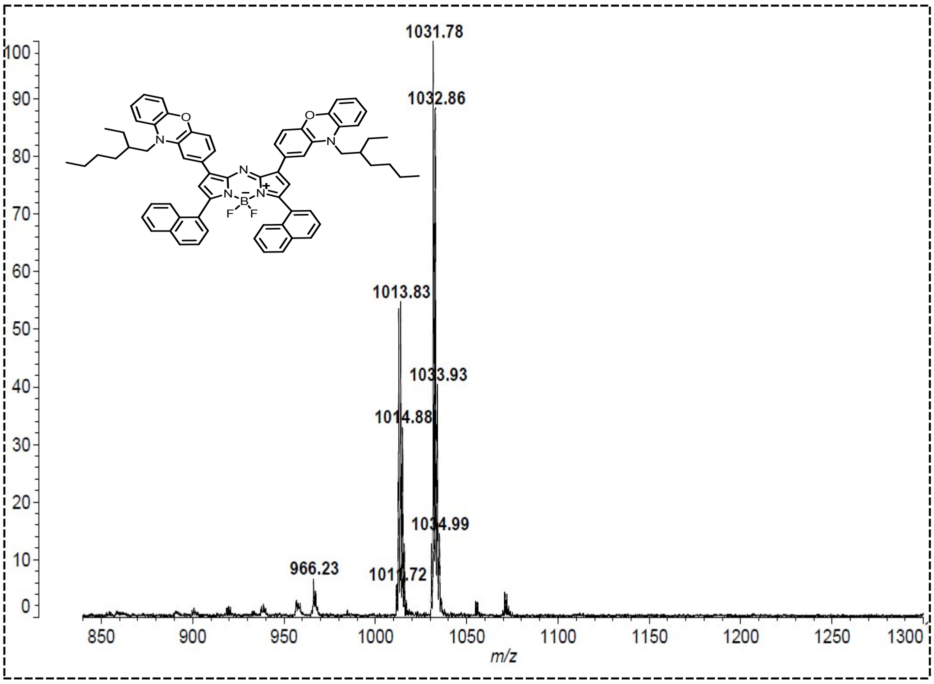

Fig. S25**:** MALDI-TOF spectrum of **AZA-POZ-BOD**

13. References:

1 K. Narayanaswamy, B. Yadagiri, A. Bagui, V. Gupta and S. P. Singh, *European J. Org. Chem.*, 2017, **2017**, 4896–4904.

2 T. Yanai, D. P. Tew and N. C. Handy, *Chem. Phys. Lett.*, 2004, **393**, 51–57.

3 S. Miertuš, E. Scrocco and J. Tomasi, *Chem. Phys.*, 1981, **55**, 117–129.

4 M. Cossi, V. Barone, R. Cammi and J. Tomasi, *Chem. Phys. Lett.*, 1996, **255**, 327–335.

5 X. Gime, J. M. Bofill and J. Gonza, *J. Comput. Chem.*, 2007, **28**, 2111–2121.

6 B. Yadagiri, K. Narayanaswamy, R. Srinivasa Rao, A. Bagui, R. Datt, V. Gupta and S. P. Singh, *ACS Omega*, 2018, **3**, 13365–13373.

7 M.J. Frisch, G.W. Trucks, H.B. Schlegel, M. Scuseria, A. Robb, J.R. Cheeseman, G. Scalmani, V. Barone, B. Mennucci, G.A. Petersson, et al. Gaussian 09, Revision B.01;Gaussian, Inc.: Wallingford, CT, 2010.

8 R. Dennington, T. Keith, J. Millam, Semichem Inc., Shawnee Mission KS, Gauss View, Version 5, 2009.

9 Y. Wang, Y. Zhang, N. Qiu, H. Feng, H. Gao, B. Kan, Y. Ma, C. Li, X. Wan and Y. Chen, *Adv. Energy Mater.*, 2018, **8**, 1–7.